Journal of Materials and Electronic Devices 4 (2022) 8-15



CdO:NiO Nanocomposite Photodiodes

Burhan COŞKUN

Kırklareli University, Faculty of Art and Science, Department of Physics, Kırklareli, Turkey

CdO:NiO solution was used to produce nanocomposite thin films which were produced in 1:1 molar rate using sol gel method. The drop casting technique was used to apply nanoparticles on p-type Si wafers and spin coating method was used after the drop cast. Optical absorption and transmission plots of the composite thin film were obtained using visible UV spectra. The energy bandgap of photodiode was calculated using UV data where bandgap energy was calculated as CdO:NiO composites. I-V data was obtained in different light intensities. Using I-V characteristics different photodiode parameters were calculated using different techniques. I-V characteristics were used to assess photovoltaic different photovoltaic characteristics such as ideality factor, barrier height, series resistance, Shunt resistance, etc. Thermionic emission theory and Cheung & Cheung function were used to assess such properties. I_{ph} and photoresponsivity characteristics were also addressed in the work. Photodiode exhibits illumination dependent characteristics where an alteration in illumination intensity alters photoresponsive characteristics.

Keywords: *CdO thin films; NiO thin films; CdO:NiO Composites; Photodetectors; Photodiodes*

Submission Date: 27 September 2022
Acceptance Date: 30 October 2022

**Corresponding author: burhan.coskun@klu.edu.tr*

1. Introduction

Thin films are primary and initial parts of the developing modern technologies [1–3]. They are mostly used in nanotechnology applications and electronic devices such as sensors, displays, detectors, etc. Organic and inorganic type films are films which were commonly reported in the literature for possible applications [4–6]. Organic films are often found to be affordable which were consisting of organic molecules such as carbon, hydrogen, nitrogen and oxygen. Therefore, they could exhibit special properties pertaining to organic molecules such as being flexible and cheap. Organic molecules are often known to be flexible; hence, the application of organic molecules to the surfaces retains their flexibility. They are often affordable since most metals are precious and are not as abundant as organic materials. On the other hand, organic thin films can have some drawbacks. For example, some organic films could be affected by external factors such as heat, humidity, etc. They cannot resist external physical effects such as press, scratch, tension, etc. Organic thin films can easily be removed from the surface and/or they can lose their performance since they can be affected by the chemical environments such as acids and alcohols. But, metallic based thin film structures were found to be resistant to external factors such as weak acids, aqueous environment, alcohol, and physical effects [7–9]. Metallic thin films also exhibit astonishing electrical, and electrochemical characteristics.; some metallic films could even illustrate magnetic properties [10–15].

Different types of metals could be found in nature, and almost all metals find an application in the electronic and optoelectronic industry. Among those, iron oxide, nickel and cobalt based films were often preferred magnetic applications [11,12,16]. Tungsten, platinum, copper and gold based films were known for their catalytic properties [17,18]. ZnO, TiO_2, CdO based films were preferred for optoelectronic, photovoltaic and photodetector applications [19–21]. CdO films show low bandgap energy, and good electrical properties with outstanding photovoltaic and

photoresponsive properties [20,22]. Therefore, they were vastly used in photovoltaic properties such as photodiodes, solar cells and photodetectors. CdO is often preferred in IR detectors therefore, they were used as additives in the optoelectronic devices to enhance the performance of the devices [9,23–25]. There is a limited effort in the literature to investigate the photovoltaic and photodiode properties of thin films. Ni based materials often exhibit ferromagnetic and/or ferrimagnetic characteristics; therefore, they were mostly used in magnetic applications [26–28]. However, there is considerable effort in the literature to assess Ni based materials as sensors or catalyser [29–31].

Mixing two different material and producing a composite help people to obtain a material with unique properties. Therefore, each composite may have unique properties and mixing two different metals at specific rates could enable us to adjust electrical properties, chemical properties, magnetic properties, catalytical properties, etc [32–35]. For example, mixing paramagnetic materials with ferromagnetic materials can give us a material with ferrimagnetic properties; on the other hand, mixing insulating materials with metals can give them conductive properties [2,36–38]. Hence, mixing different materials at different rates is preferred in optoelectronic applications to adjust electrical and optoelectronic properties such as conductivity, capacitance, photoresponse, photocurrent, etc.

In this work, we produced CdO:NiO thin films by mixing them 1:1 molar ratio using sol gel method. The solution was drop cast on a p-type Si wafer and spin coated. Al contacts were obtained to have good contact. Where Al/p-Si/CdO:NiO/Al photodiodes were produced. I-V characteristics were obtained under different illumination Diode characteristics were calculated using this data. Bandgap energies of the thin films were calculated using UV visible spectra where increased ZnO dopant decrease the bandgap energies of TiO_2 photodiodes.

2. Experimental

2.1. Production of ZnO doped TiO_2 gels

The sol-gel nanoparticle production protocols were used in the production of CdO:NiO photodetectors. 0.5M Cadmium acetate (Cd(Ac) were dissolved in 10ml 2-methoxyethanol a beaker; and 0.5M Nickel (II) Chloride (Hexahydrate) were dissolved in 10ml 2-methoxyethanol in another beakers. Magnetic shaker shakes each beaker for 10 mins. 0.5ml CdO solution was added to 0.5 ml NiO where CdO:NiO solutions in 1:1 molar rate were obtained.

2.2. Production of CdO:NiO nanocomposite photodiodes

P-type Si substrates were chemically cleaned before the coating procedure. In the cleaning process, residual dirt Si wafers were stirred using deionized water. Sonication was applied to the p-type silicon wafers for 5 mins in deionized water. Si wafer was then sonicated in ethanol for 5 mins and sonicated in deionized water. Lastly, HF:H_2O (1:10ml) were prepared and sonicated for 5 mins and washed using pure water [39]. Samples were then dried using N_2 gas. 2 cm x 2 cm wafers were cut; 6 layers of film were then spin coated on substrates. Spin coating was applied at 3000 rpm for 30 secs for each layer. Each layer was dried on a hot plate for 2 mins the temperature of which is 100 ˚C. 6 layers were applied. At 420 ˚C, film coated substrates were annealed for 1h. When the coating procedure was finished, Al contact was applied using a thermal evaporator. The coating was applied at 2 - 4 A˚/s evaporation rate. Total of 100 nm contact was coated and photodetectors in Al/p-Si/CdO:NiO/Al photodetectors were formed. The result products were then annealed at 570 ˚C for 5 mins under N_2 gas. FYTRONIX FY-7000 were used in the investigations. Shimadzu 3600 UV/VIS spectrometer was used in the assessment of optic properties [40].

3. Results

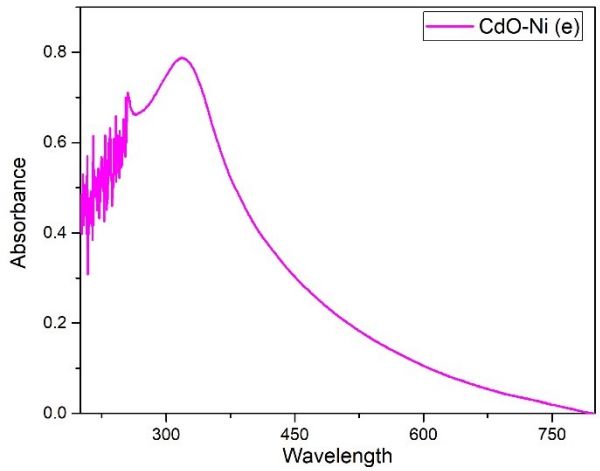
3.1. Optic Properties

Optic properties of the photodetectors illustrated in Figure 1 where Abs - wavelength (a), Abs – hυ (d) characteristics were presented. It was seen in Figure 1a and Figure 1b that Al/p-Si/CdO:NiO/Al photodetectors show high absorbance in UV range and absorbance starts to diminish in visible range. Using absorbance data, E_g (energy bandgap) of the thin films were determined. Following formula was used in the calculations

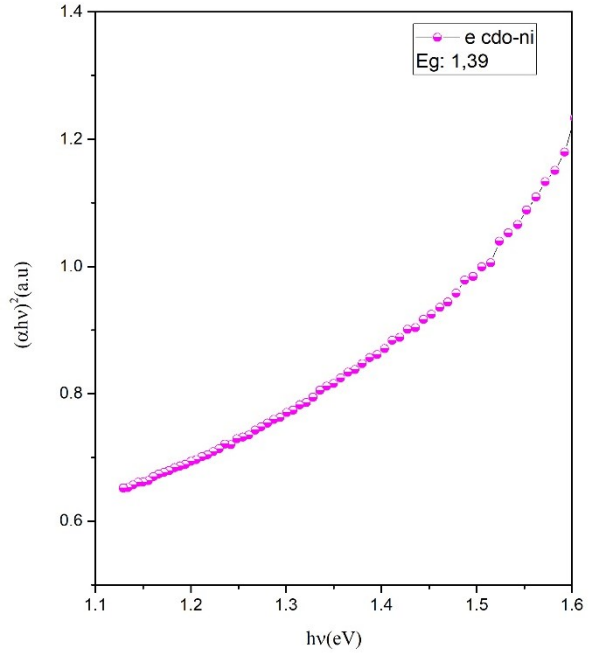
$$\alpha h\nu = A(h\nu - Eg)^n \qquad (1)$$

where $\alpha = F(R)/d$, A is a constant, d is the thickness of thin films, E_g is band gap energy, n is a constant which determines the optic transfer. Two different kinds of transfer may be observed: direct transfers (i) indirect transfers (ii). Indirect transfers were determined as n=1/2, 3/2, 5/2… while direct transfers were determined as n=1, 2, 3…

$(\alpha h\nu)^2$ –hν characteristics were illustrated in Figure 1b where E_g of Al/p-Si/CdO:NiO/Al photodetectors were found as 1.39 eV.



-a-



-b-

Figure 1. Abs - wavelength (a) and $(\alpha hv)^2$ –hv (b) characteristics of Al/p-Si/CdO:NiO/Al photodetectors.

3.1. Photoresponsive Properties

I – V (current- voltage) characteristics of the Al/p-Si/CdO:NiO/Al photodiodes were assessed between -2V and 3V. I – V characteristics were presented in Figure 2. In the measurement, I-V characteristics were obtained in dark, 20mW/c^2, 40mW/cm^2, 60mW/cm^2, 80mW/cm^2, and 100mW/cm^2. It was seen that the photodiode is responsive to the light where different photocurrent was obtained for different illumination intensities. Regarding the I-V graph, it is clear that Al/p-Si/CdO:NiO/Al photodiode is responsive to the light and exhibits photodiode characteristics. Since there is an apparent difference between forward bias and reverse bias in the plot where the measured current clearly alters. Therefore, we can say that Al/p-Si/CdO:NiO/Al photodiode structures exhibit diode characteristics. The I-V graph also shows that photodiodes are responsive to applied light. It was seen that illumination intensity change in the light alters measured photocurrent. However, no apparent relation was observed between the light intensity and measured photocurrent. Different diode parameters such as ideality factor (n), reverse saturation current, barrier height (Φ_B) series resistance (R_s), etc. were calculated using Cheung & Cheung method and thermionic emission theory.

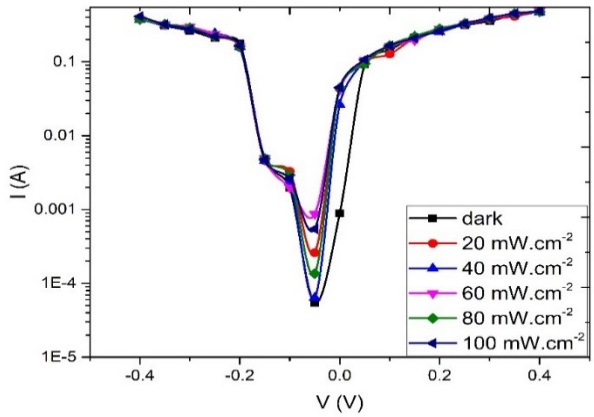


Figure 2. I-V characteristics of Al/p-Si/CdO:NiO/Al photodiodes.

In common Thermionic Emission theory calculations following equation was used to assess I-V plots:

$$I = AA^*T^2 \exp\left(\frac{-q\,\Phi_B}{kT}\right)\left[\exp\left(\frac{q(V-IR_S)}{kT}\right) - 1\right] \qquad (2)$$

where A is the active surface area of the diode, A* is the Richardson constant, q is the charge of the electron, k is the Boltzmann constant, V is the potential, R_s is the serries resistance, T is the Kelvin temperature, Φ_B is the barrier height

Equation 1 when V-IR$_s$>>3kT

$$I=I_0 \exp\left(\frac{qV}{nkT}\right) \qquad (3)$$

$$I_0=AA^*T^2 \exp\left(\frac{-q\,\Phi_B}{kT}\right) \qquad (4)$$

Eq 5 is obtained by taking derivative of V after taking the logarithm of Equation 3.

$$n=\frac{q}{kT}\frac{d(v)}{d(\ln(I))} \qquad (5)$$

ln(I) against V in the low and medium voltage region is calculated together with other constants, the ideality factor n is found. The graph of ln(I) against V intersects ln(I) gives reverse saturation current. Here, Equation 4 gives the barrier height.

In Cheung & Cheung method, the barrier height, diode resistance Rs, and ideality factor are determined using following equations:

$$\frac{dV}{dln(I)} = IR_s + \frac{nkT}{q} \quad (6)$$

$$H(I) = V - \frac{nkT}{q} \ln\left(\frac{I}{AA^*T^2}\right) \quad (7)$$

$$H(I) = IR_s + n\,\Phi_B \quad (8)$$

Using the equations above the graph of d(V)/d(ln(I)) and H(I) against I is drawn using the values in the low and medium voltage region of the I-V graph. Here, the ideality factor *n* was calculated using the d(V)/d(ln(I)) against I. Φ_B was derived from *n* where the curve cuts the y axis in the H(I) graph. The slope of the curve gives the R_s value.

Table 1. Diode parameters obtained via thermionic emission theory.

Illumination Intensity	Ideality Factor (n)	Barrier Height (Φ_B)	Reverse saturation current I_o
0	4.22	0.38	0.058
20	8.34	0.37	0.080
40	4.06	0.38	0.063
60	4.37	0.37	0.067
80	3.35	0.38	0.052
100	4.44	0.37	0.069

Table 2. Diode parameters obtained via Ohm's law and Cheung & Cheung theory.

Illumination Intensity	Ohm's law		Cheung&Cheung Function	
	Rs (Ohm)	Shunt Resistance (Ohm)	Ideality Factor (n)	Rs (Ohm)
0	0.85	17.75	13.41	0.54
20	0.73	16.26	8.31	0.47
40	1.77	22.96	9.67	0.18
60	1.23	16.88	5.63	0.52
80	1.80	25.18	1.93	0.79
100	1.56	23.87	1.11	0.80

Diode parameters obtained using the thermionic emission theory was presented in Table 1. Ideality factors were found between 3.35 and 8.34. It was seen that ideality factors alter with the altering illumination intensity. Cheung & Cheung method provides an ideality factor between 1.11 and 13.41. It was again seen ideality factor seem to exhibit decreasing trend with increasing illumination intensity where the ideality factor of 13.41 was obtained at dark measurement, and the ideality factor of 1.11 was obtained for measurement at 100 mW/cm^2. It should be noted that enhanced illumination enhanced the diode characteristics in Cheung & Cheung approximation. It was expected to see the ideality factor as 1 which corresponds to an optimum diode. However, ideality factors bigger than 1 were often reported in the literature. For example, Aslan et al. find the ideality factor of ZnO doped carbon photodiodes between 3.76 and 6.37; Koc reported the ideality factor of CuO doped carbon photodiodes 3.74. Aslan et al find the ideality factor of Ti doped amorphous carbon photodiodes as 3.17 and 1.84; Ilhan et al find the ideality factor of Cd doped TiO_2 solar detectors between 5.75 and 7.86; Ilhan et al find the ideality factor of $CuNiSnS_4$ as 5.84 [2,15,21,37,41]. Ideality factors obtained using the Cheung & Cheung method and thermionic emission theory was presented in Figure 3.

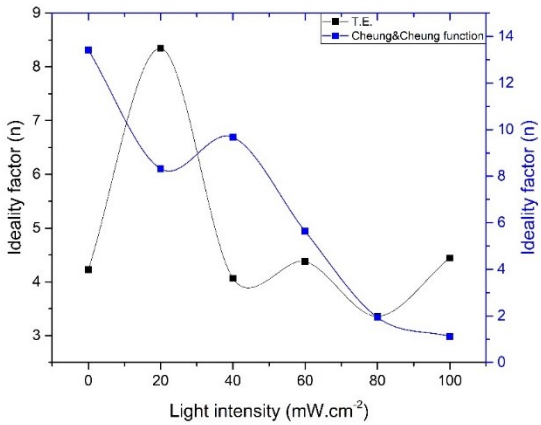


Figure 3. Ideality factors obtained using Cheung & Cheung method and thermionic emission theory for Al/p-Si/CdO:NiO/Al photodiodes.

Barrier height was also calculated for Al/p-Si/CdO:NiO/Al photodiodes. The barrier height was found around 0.32 eV. The barrier height was not altered with the external illumination. Barrier heights are strongly dependent on diode structure. Therefore, different barrier heights were reported in the literature pertaining to different diodes. For example, Aslan et al. find the barrier height of ZnO doped carbon photodiodes between 0.48 eV and 0.56 eV; Koc reported the barrier height of CuO doped carbon photodiodes between 0.47 eV and 0.56 eV. Aslan et al find the barrier height of Ti doped amorphous carbon photodiodes as 0.46 eV and 0.56 eV; Ilhan et al find the barrier height of Cd doped TiO_2 solar detectors between 0.48 eV and 0.50 eV;

Ilhan et al find the barrier height of $CuNiSnS_4$ as 0.47 eV [2,15,21,37,41]. It was seen that both the ideality factor and barrier height of Al/p-Si/CdO:NiO/Al photodiodes were found coherent with the results reported in the literature. Reverse saturation current (I_0) is an important diode parameter which was often used to identify and characterize the diode characteristics. In our case reverse saturation current related parameters were calculated using thermionic emission theory which was presented in Table 1. The reverse saturation current was found between 0.058A and 0.080 A. It was seen that the reverse saturation current alters with altering illumination. However, no direct correlation between illumination intensity and measured reverse saturation was observed for Al/p-Si/CdO:NiO/Al photodiodes. Reverse saturation current and calculated barrier height values depending on altering illumination intensity for Al/p-Si/CdO:NiO/Al photodiodes were presented in Figure 4.

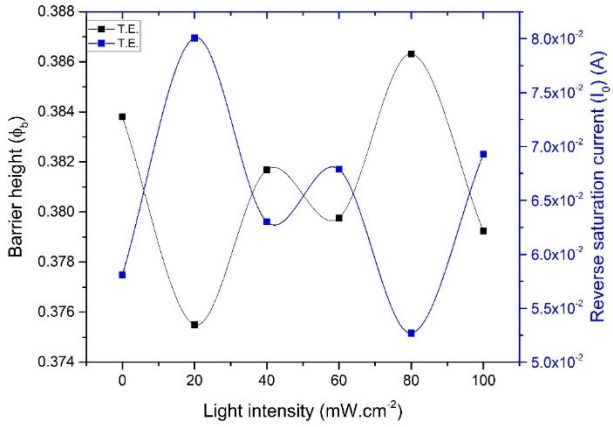


Figure 4. Barrier Height and measured reverse saturation values for Al/p-Si/CdO:NiO/Al photodiodes.

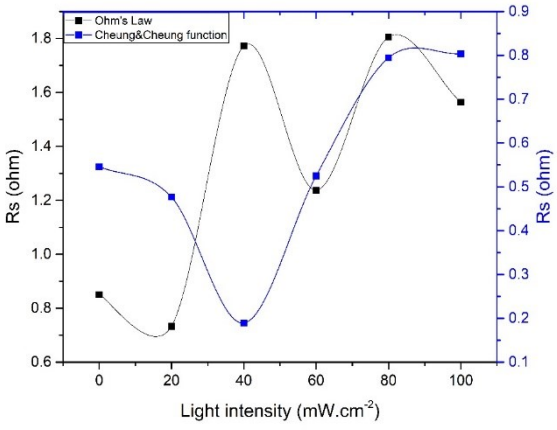


Figure 5. R_s values obtained using Ohm's law and Cheung & Cheung function for Al/p-Si/CdO:NiO/Al photodiodes.

Serries resistance (R_s) values are important electrical parameters for photodiodes. They often used to identify the diode characteristics. It is important to identify the Rs characteristics to used diodes in device applications. In our research we calculated R_s values of Al/p-Si/CdO:NiO/Al photodiodes using Ohm's law and Cheung & Cheung function. Rs value was calculated between 0.73 Ohm and 1.77 Ohm. It was seen that relatively higher Rs values were obtained under illumination for Al/p-Si/CdO:NiO/Al photodiodes using Ohm's law. Similar values were calculated using Cheung & Cheung function where R_s value between 0.18 Ohm and 0.80 Ohm was found. R_s values were found quite identical where no apparent R_s difference was observed for the measurement obtained under illumination and dark. Light intensity related graphs showing the R_s values obtained using two different methods were presented in Figure 5.

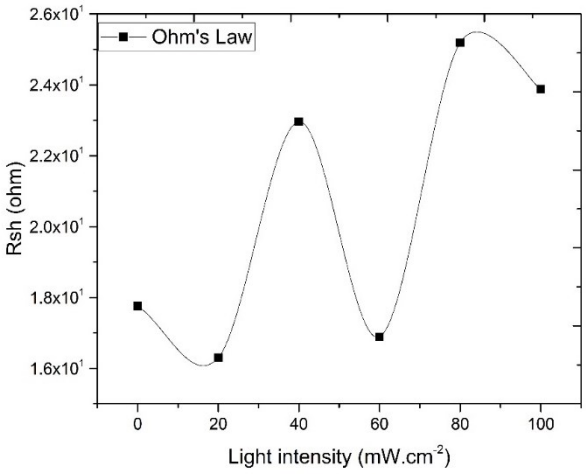


Figure 6. R_{sh} values obtained using Ohm's law for Al/p-Si/CdO:NiO/Al photodiodes.

Shunt resistance (R_{sh}) was also calculated using Ohm's law. Shunt resistance values were presented in Table 2 and Figure 6. It was seen that Shunt resistance alters with light the application of an external light where no direct correlation was observed.

Lastly, we calculated the photoresponsivity and photocurrent properties of our diodes. It was seen that measured photocurrent alters with altering illumination intensity. In reverse bias, no direct relation between illumination intensity and measured photocurrent could be seen. On contrary, enhancing photocurrent was obtained for enhancing illumination intensity for the forward bias. Similarly, photoresponsivity was also assessed for the Al/p-Si/CdO:NiO/Al photodiodes. It was seen that no direct relationship between illumination intensity and photoresponsivity was observed for the reverse bias zone. For forward bias, decreased responsivity was observed for increasing illumination intensity was seen. We found that

illumination intensity negatively affects the photoresponsivity for Al/p-Si/CdO:NiO/Al photodiodes.

Table 3. Light intensity related diode photosensitivity and photocurrent parameters.

I_{ph} (A)					
Volt	**20 mW.cm^{-2}**	**40 mW.cm^{-2}**	**60 mW.cm^{-2}**	**80 mW.cm^{-2}**	**100 mW.cm^{-2}**
-0.30000001	0.024031	0.013106	0.033326	0.024882	0.01515
0.300000012	0.019548	0.027074	0.03177	0.035761001	0.036443
R (A.W^{-1})					
-0.30000001	258.3978533	70.46236664	119.448	66.88709777	32.58065
0.300000012	210.1935515	145.559142	113.871	96.13172186	78.37204

3. Results

In our work, we produced Al/p-Si/CdO:NiO/Al photodiodes. Moreover, we investigated diode parameters and photovoltaic and photoresponsive characteristics of the Al/p-Si/CdO:NiO/Al photodiodes. I-V characteristics illustrated that Al/p-Si/CdO:NiO/Al structures exhibit photodiode characteristics. It was seen that diode parameters such as ideality factor, barrier height, series resistance, and shunt resistance were affected by external illumination. It was seen that external light alters such parameters but no clear correlation between such parameters and external illumination was found. Ideality factor and barrier height values were compared with the results previously reported in the literature and seen that our results were within the acceptable range. Lastly, photoresponsive characteristics exhibit decreasing characteristics with enhancing illumination intensity. Such a case indicates that our photodiodes are not suitable for solar tracking applications.

Acknowledgement

I would like to thank Dr. Ayşegül Dere, Dr.. Mümin Mehmet Koç, Dr. Mustafa İlhan and Dr. Fatih Ünal for their support in this work. I also would like to acknowledge the support of Kirklareli University Scientific Research Coordination Office with project number 230.

References

[1] Y. Takaoka, T. Sakamoto, S. Tsukiji, M. Narazaki, T. Matsuda, H. Tochio, M. Shirakawa, I. Hamachi, Self-assembling nanoprobes that display off/on 19F nuclear magnetic resonance signals for protein detection and imaging, Nat. Chem. 1 (2009) 557–561. doi:10.1038/nchem.365.

[2] N. Aslan, M.M. Koç, A. Dere, B. Arif, M. Erkovan, A.G. Al-Sehemi, A.A. Al-Ghamdi, F. Yakuphanoglu, Ti doped amorphous carbon (Al/Ti-a:C/p-Si/Al) photodiodes for optoelectronic applications, J. Mol. Struct. 1155 (2018) 813–818. doi:10.1016/j.molstruc.2017.11.050.

[3] F.J. González, B. Ilic, J. Aida, G.D. Boreman, Antenna-coupled infrared detectors for imaging applications, IEEE J. Sel. Top. Quantum Electron. 11 (2005) 117–120. doi:10.1109/JSTQE.2004.841474.

[4] A. Dere, M. Soylu, F. Yakuphanoglu, Solar light sensitive photodiode produced using a coumarin doped bismuth oxide composite, Mater. Sci. Semicond. Process. 90 (2019) 129–142. doi:10.1016/j.mssp.2018.10.009.

[5] A. Mekki, A. Dere, K. Mensah-Darkwa, A. Al-Ghamdi, R.K.K. Gupta, K. Harrabi, W.A.A. Farooq, F. El-Tantawy, F. Yakuphanoglu, Graphene controlled organic photodetectors, Synth. Met. 217 (2016) 43–56. doi:10.1016/j.synthmet.2016.03.015.

[6] P.D. Rack, P.H. Holloway, The structure, device physics, and material properties of thin film electroluminescent displays, Mater. Sci. Eng. R Reports. 21 (1998) 171–219. doi:10.1016/S0927-796X(97)00010-7.

[7] D. Ponnusamy, A.K. Prasad, S. Madanagurusamy, CdO-TiO2 nanocomposite thin films for resistive hydrogen sensing, Microchim. Acta. 183 (2016) 311–317. doi:10.1007/s00604-015-1653-y.

[8] K.C. Liddiard, Thin-film resistance bolometer IR detectors, Infrared Phys. 24 (1984) 57–64. doi:10.1016/0020-0891(84)90048-4.

[9] S. Özden, M.M. Koc, Spectroscopic and microscopic investigation of MBE-grown CdTe (211)B epitaxial thin films on GaAs (211)B substrates, Appl. Nanosci. 8 (2018) 891–903. doi:10.1007/s13204-018-0727-7.

[10] M. Mahdi, A. Djabri, M.M. Koc, R. Boukhalfa, M. Erkovan, Y. Chumakov, F. Chemam, Ab initio study of GdCo5 magnetic and magneto-optical properties, Mater. Sci. Pol. 37 (2019) 182–189. doi:10.2478/msp-2019-0017.

[11] M. Erkovan, M.E. Aköz, U. Parlak, O. Öztürk, The Study of Exchange Bias Effect in PtxCo1−x/CoO Bilayers, J. Supercond. Nov. Magn. 30 (2017) 2909–2913. doi:10.1007/s10948-017-4127-0.

[12] M. Yaqoob Khan, C. Bin Wu, M. Erkovan, W. Kuch, Probing antiferromagnetism in NiMn/Ni/(Co)/Cu3Au(001) single-crystalline epitaxial thin films, J. Appl. Phys. 113 (2013) 023913. doi:10.1063/1.4775575.

[13] M.M.K. Mustafa İlhan, Infrared Sensing Properties of Quaternary Cu2CoSnS4 Photodetectors, J. Mater. Electron. DEVICES. 1 (2020) 19–24.

[14] M. İlhan, M.M. Koç, B. Coşkun, A. Dere, F. Yakuphanoğlu, Structural and optoelectronic characterization of Cu2CoSnS4 quaternary functional photodetectors, Optik (Stuttg). 212 (2020) 164724. doi:10.1016/j.ijleo.2020.164724.

[15] M. İlhan, M.M. Koç, B. Coşkun, F. Yakuphanoğlu, Optical, Electrical and Photoresponsive Properties of Cu2NiSnS4 Solar Detectors, J. Electron. Mater. 49 (2020) 4457–4465. doi:10.1007/s11664-020-08197-5.

[16] A. Djabri, M. Mahdi, R. Boukhalfa, M. Erkovan, Y. Chumakov, F. Chemam, Structural, Magnetic, and Magneto-Optical Properties of Fe/Cu Superlattices, J. Supercond. Nov. Magn. 30 (2017) 3207–3214. doi:10.1007/s10948-017-4128-z.

[17] S.J. Ippolito, S. Kandasamy, K. Kalantar-Zadeh, W. Wlodarski, Hydrogen sensing characteristics of WO3 thin film conductometric sensors activated by Pt and Au catalysts, in: Sensors Actuators, B Chem., Elsevier, 2005: pp. 154–158. doi:10.1016/j.snb.2004.11.092.

[18] R. Yang, J. Leisch, P. Strasser, M.F. Toney, Structure of dealloyed PtCu3 thin films and catalytic activity for oxygen reduction, Chem. Mater. 22 (2010) 4712–4720. doi:10.1021/cm101090p.

[19] M. Soylu, B. Coskun, A.G. Al-Sehemi, A.A. Al-Ghamdi, F. Yakuphanoglu, The validity of Kohlrausch law for the photocurrent transient and the role of N2/Ar flow ratio in photoconductivity of sputtered CoZnO, J. Alloys Compd. 712 (2017) 152–163. doi:10.1016/j.jallcom.2017.04.041.

[20] F. Yakuphanoglu, Transparent metal oxide films based sensors for solar tracking applications, Compos. Part B Eng. 92 (2016) 151–159. doi:10.1016/j.compositesb.2016.02.039.

[21] M. İlhan, M.M. Koç, B. Coşkun, M. Erkovan, F. Yakuphanoğlu, Cd dopant effect on structural and optoelectronic properties of TiO2 solar detectors, J. Mater. Sci. Mater. Electron. 32 (2021) 2346–2365. https://link.springer.com/article/10.1007/s10854-020-05000-3 (accessed March 9, 2021).

[22] B.A.H. Ameen, A. Yildiz, W.A. Farooq, F. Yakuphanoglu, Solar Light Photodetectors Based on Nanocrystalline Zinc Oxide Cadmium Doped/p-Si Heterojunctions, Silicon. 11 (2019) 563–571. doi:10.1007/s12633-017-9656-4.

[23] A. Rogalski, Infrared detectors: An overview, Infrared Phys. Technol. 43 (2002) 187–210. doi:10.1016/S1350-4495(02)00140-8.

[24] W. Lei, J. Antoszewski, L. Faraone, Progress, challenges, and opportunities for HgCdTe infrared materials and detectors, Appl. Phys. Rev. 2 (2015) 041303. doi:10.1063/1.4936577.

[25] E. Bilgilisoy, S. Özden, E. Bakali, M. Karakaya, Y. Selamet, Characterization of CdTe Growth on GaAs Using Different Etching Techniques, J. Electron. Mater. 44 (2015) 3124–3133. doi:10.1007/s11664-015-3830-5.

[26] A. Sharma, B.K. Lee, Photocatalytic reduction of carbon dioxide to methanol using nickel-loaded TiO2 supported on activated carbon fiber, Catal. Today. 298 (2017) 158–167. doi:10.1016/j.cattod.2017.05.003.

[27] Z. Jiang, J. Xie, D. Jiang, X. Wei, M. Chen, Modifiers-assisted formation of nickel nanoparticles and their catalytic application to p-nitrophenol reduction, CrystEngComm. 15 (2013) 560–569. doi:10.1039/c2ce26398j.

[28] M. Erkovan, Y.A. Shokr, D. Schiestl, C.B. Wu, W. Kuch, Influence of NixMn1−x thickness and composition on the Curie temperature of Ni in NixMn1−x/Ni bilayers on Cu3Au(001), J. Magn. Magn. Mater. 373 (2015) 151–154. doi:10.1016/J.JMMM.2014.02.017.

[29] M. Mokarram, A. Saber, R. Obeidi, Effects of heavy metal contamination released by petrochemical plants on marine life and water quality of coastal areas, Environ. Sci. Pollut. Res. 28 (2021) 51369–51383. doi:10.1007/S11356-021-13763-3/FIGURES/9.

[30] E. Hasanoğlu Özkan, N. Aslan, M.M. Koç, N. Kurnaz Yetim, N. Sarı, Fe3O4 nanoparticle decorated novel magnetic metal oxide microcomposites for the catalytic degradation of 4-nitrophenol for wastewater cleaning applications, J. Mater. Sci. Mater. Electron. 33 (2022) 1039–1053. doi:10.1007/S10854-021-07376-2/TABLES/1.

[31] N. KURNAZ YETİM, Hidrotermal olarak Sentezlenen Çiçek benzeri NiO@Fe3O4'ün Katalitik Özellikleri, Düzce Üniversitesi Bilim ve Teknol. Derg. 8 (2020) 1964–1974. doi:10.29130/dubited.721970.

[32] A. Gencer Imer, Investigation of Al doping concentration effect on the structural and optical properties of the nanostructured CdO thin film, Superlattices Microstruct. 92 (2016) 278–284. doi:10.1016/J.SPMI.2016.01.035.

[33] R.K.K. Gupta, F. Yakuphanoglu, F.M.M. Amanullah, Band gap engineering of nanostructure Cu doped CdO films, Phys. E Low-Dimensional Syst. Nanostructures. 43 (2011) 1666–1668. doi:10.1016/J.PHYSE.2011.05.019.

[34] B. Coskun, Capacitance and Dielectric Properties of Mn Doped CdO Photodetectors, J. Mater. Electron. DEVICES. 1 (2019) 65–71.

[35] R. Karaçam, N.K. Yetim, M.M. Koç, Structural and Magnetic Investigation of Bi2S3@Fe3O4 Nanocomposites for Medical Applications, J. Supercond. Nov. Magn. 33 (2020) 2715–2725.

https://doi.org/10.1007/s10948-020-05518-x (accessed August 27, 2020).

[36] A. Kösemen, Z. Alpaslan Kösemen, B. Canimkubey, M. Erkovan, F. Başarir, S.E. San, O. Örnek, A.V. Tunç, Fe doped TiO2 thin film as electron selective layer for inverted solar cells, Sol. Energy. 132 (2016) 511–517. doi:10.1016/j.solener.2016.03.049.

[37] M. Koç, N. Aslan, M. Erkovan, B. Aksakal, O. Uzun, W. Aslam, F. Yakuphanoğlu, Electrical characterization of solar sensitive zinc oxide doped-amorphous carbon photodiode, Optik (Stuttg). 178 (2019) 316–326. doi:https://doi.org/10.1016/j.ijleo.2018.10.008.

[38] N. Kurnaz Yetim, N. Aslan, M.M. Koç, Structural and catalytic properties of Fe3O4 doped Bi2S3 novel magnetic nanocomposites: P-Nitrophenol case, J. Environ. Chem. Eng. 8 (2020) 104258. doi:10.1016/j.jece.2020.104258.

[39] S. Özden, M.M. Koç, Wet-chemical etching of GaAs(211)B wafers for controlling the surface properties, Int. J. Surf. Sci. Eng. 13 (2019) 79. doi:10.1504/IJSURFSE.2019.102359.

[40] S. UYAR, B. COŞKUN, M. İLHAN, M.M. KOC, Optoelectronic Properties of ZnO:TiO2 Nanocomposite Thin Films, J. Mater. Electron. DEVICES. 5 (2021) 21–27. http://dergi-fytronix.com/index.php/jmed/article/view/140 (accessed October 15, 2021).

[41] M.M. Koc, Photoelectrical properties of solar sensitive CuO doped carbon photodiodes, J. Mol. Struct. 1208 (2020) 127872. doi:10.1016/j.molstruc.2020.127872.

[42] N. Aslan, N. Başman, O. Uzun, M. Erkovan, F. Yakuphanoğlu, The effects of deposition potential on the optical, morphological and mechanical properties of DLC films produced by electrochemical deposition technique at low, Mater. Sci. 37 (2019) 166–172. doi:10.2478/msp-2019-0023.